

A decorative graphic at the top of the page features several colorful, three-dimensional nanostructures (resembling helices or spheres with internal patterns) arranged along diagonal lines. A red line connects some of these structures, suggesting a path or sequence. The background is a light blue gradient.

# Novel nanostructures for SERS biosensing

Surface-enhanced Raman scattering (SERS) is a powerful analytical tool for chemical and biological sensing applications. However, one feature which has limited its use in biosensing applications is the difficulty involved in producing uniform, highly sensitive, and reproducible SERS substrates. Recent developments in oblique angle deposition and other nanofabrication techniques have overcome this limitation, providing an unprecedented opportunity to develop SERS substrates for pathogen biosensor applications. Recently reported examples of SERS's newfound sensing abilities include the capacity to detect low levels of viruses and bacteria, as well as to discriminate between types and strains of pathogens, including pathogens with gene deletions. A brief review of our recent progress in SERS biosensing is given in this article.

Ralph A. Tripp<sup>1</sup>, Richard A. Dluhy<sup>2</sup>, and Yiping Zhao<sup>3\*</sup>

<sup>1</sup>Department of Infectious Diseases, University of Georgia, Athens, GA 30602, USA

<sup>2</sup>Department of Chemistry, University of Georgia, Athens, GA 30602, USA

<sup>3</sup>Department of Physics and Astronomy, University of Georgia, Athens, GA 30602, USA

\*E-mail: [zhaoy@physast.uga.edu](mailto:zhaoy@physast.uga.edu)

The rapid and sensitive detection of pathogens is critical for disease intervention strategies, as well as the control and prevention of pandemics and acts of bioterrorism. There is a need to be able to perform pathogen detection, both in laboratory facilities, and under field conditions. Consequently, biosensing platform technologies are under development to allow for both applications. Current methods of virus and bacteria detection generally employ antibody-based assays such as enzyme-linked immunosorbant assays (ELISA), fluorescent antibody assays<sup>1</sup>, or serologic evaluation for exposure<sup>2</sup>. Many of these

assay methods provide only a limited level of sensitivity, thus low level pathogen detection generally requires nucleic acid amplification coupled with polymerase chain reaction (PCR) assays<sup>3</sup>.

More recently, other diagnostic methods such as microcantilevers<sup>4</sup>, evanescent wave biosensors<sup>5</sup>, immunosorbant electron microscopy<sup>6</sup>, and atomic force microscopy<sup>7</sup> have been investigated to overcome some of the limitations of sensitivity, but these new techniques are unable to effectively discriminate between types and/or species of pathogen with reasonable sample throughput. The research

directions for improvement of biosensing methods require reduction or elimination of sample preparation or amplification procedures. Detection and discrimination of specimens in complex biological media are also a necessity, together with reproducible results, cost and time effectiveness, and ease of use under most conditions.

### SERS detection dictated by substrate fabrication

Surface-enhanced Raman scattering (SERS) has emerged as a powerful analytical tool that extends the possibilities of vibrational spectroscopy to solve a vast array of chemical and biochemical problems. SERS is an extension and variation of standard Raman spectroscopy, a vibrational spectroscopic technique that provides detailed information about the materials under investigation at the molecular level<sup>8</sup>. Since the discovery of the SERS effect in the 1970s<sup>9–11</sup>, SERS has been applied to a wide variety of analytical applications, including biochemistry and the life sciences<sup>12</sup>. As has been reviewed in detail elsewhere<sup>13–20</sup>, two primary mechanisms are believed to be responsible for SERS enhancement: a long-range classical electromagnetic (EM) effect<sup>20</sup> and a short-range chemical (CHEM) effect<sup>21</sup>. These two mechanisms contribute simultaneously to the overall enhancement; EM is thought to contribute the most ( $\sim 10^4$ – $10^7$ ) to the observed intensity enhancement, while CHEM is thought to contribute a lesser amount ( $\sim 10$ – $10^2$ ).

Since SERS is useful for determining molecular structural information and also provides ultrasensitive detection limits, including single molecule sensitivity<sup>22,23</sup>, it has been used to detect pathogens that include bacteria<sup>24</sup> and viruses<sup>25</sup>. There are two principle SERS configurations that have been used in biosensing, intrinsic or extrinsic, as shown in Fig. 1. In intrinsic detection (Fig. 1a), the analyte can be directly applied to the nanostructured surfaces and the inherent Raman spectrum of the biomolecule directly measured to identify the specimen. To allow for capture and to aid specificity of detection, antibodies, aptamers, or related molecules can be immobilized onto nanostructured surfaces as shown in Fig. 1b, and the Raman spectral differences before and after capture of the specimen can be used to identify the species. In extrinsic detection, a Raman reporter molecule is used to generate a signal for detection. For example, a Au nanoparticle may be used as the SERS-active substrate to which a Raman reporter molecule is immobilized (Fig. 1c). By coating this structure with another layer of dielectrics such as  $\text{SiO}_2$ ,  $\text{TiO}_2$ , or a polymer, a core-shell complex is formed in which the outer-shell may be decorated with capture molecules such as antibodies. Thus, specimens may be captured and detected via a sandwich structure as shown in Fig. 1c. This extrinsic SERS detection method has been successfully used for *in vivo* SERS imaging of unique or rare cancer cells<sup>26–28</sup>.

The remarkable analytical sensitivity of SERS has yet to be translated into the development of widely accepted, commercially

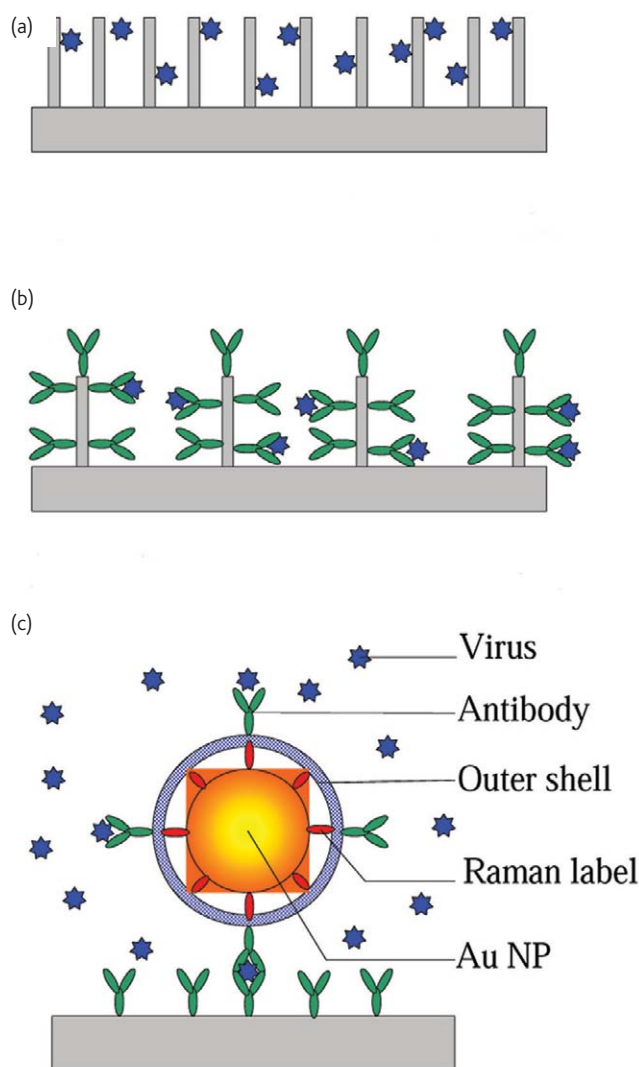


Fig. 1 Different SERS detection configurations: (a) Direct intrinsic detection; (b) indirect intrinsic detection; and (c) extrinsic detection.

viable diagnostic applications, due in large part to the difficulty in preparing robust, metal-coated substrates of the correct surface morphology that provide maximum SERS enhancements<sup>20</sup>. Some of the important requirements for an ideal SERS substrate in practical diagnostic applications are that the substrate produces a high enhancement, generates a reproducible and uniform response, has a stable shelf-life, and is simple to fabricate.

Many substrate preparation techniques exist that can form roughened metal surfaces of the types required for ideal SERS enhancements. These methods include roughening of a surface by oxidation-reduction cycles (ORC)<sup>9</sup>, metal colloid hydrosols<sup>29</sup>, laser ablation of metals by high-power laser pulses<sup>30</sup>, chemical etching<sup>31</sup>, roughened films prepared by Tollen's reagent<sup>32</sup>, photodeposited Ag films on  $\text{TiO}_2$ <sup>32</sup>, and vapor-deposited Ag metal films<sup>33–36</sup>. While the majority of substrate preparation techniques reported to date focus

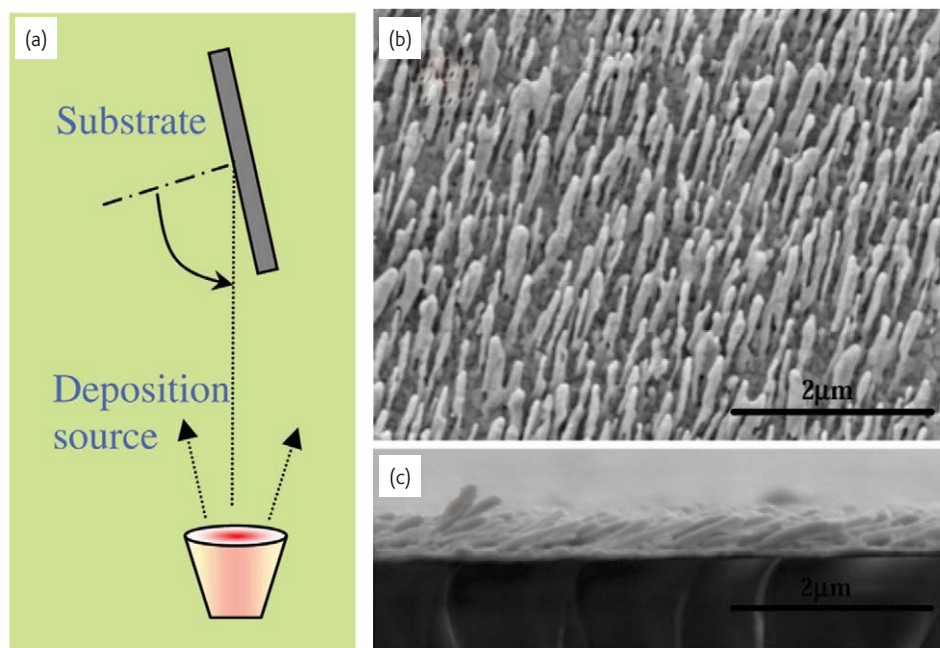


Fig. 2 (a) Schematic of oblique angle deposition. (b) Top view, and (c) cross-sectional view scanning electron micrographs of the Ag nanorod array SERS substrates.

on the problem of achieving large SERS enhancements, the other requirements listed above for the production of a practical SERS sensing substrate are seldom addressed. Currently, there are five fabrication techniques that could potentially produce the desired SERS substrates to meet these requirements: electron beam lithography, nanosphere lithography, the template method, the hybrid method, and an oblique angle vapor deposition method.

The electron beam lithography (EBL) method is an ideal method for producing uniform and reproducible SERS substrates<sup>37–41</sup>. Unfortunately, it is very expensive to produce large area substrates using EBL, unless the technique is combined with a nanoimprint lithography method<sup>42</sup>. The nanosphere lithography (NSL) method pioneered by Van Duyne and coworkers<sup>43–47</sup> involves evaporating Ag onto preformed arrays of nanopore masks by colloid particles, which are subsequently removed, leaving behind the Ag metal deposited in the interstices to form a regular Ag nanoparticle array. The template

method utilizes a nanotube-like array, such as anodized  $\text{Al}_2\text{O}_3$ , as a template to deposit Ag or Au nanorods directly into the channels via an electrochemical plating method<sup>48–53</sup>. Hybrid methods fabricate SERS substrates by depositing metal particles onto nanoporous scaffolds such as porous silicon, nanorod arrays, etc<sup>54–61</sup>. The oblique angle deposition (OAD) method is based on a conventional physical vapor deposition principle and can be used to fabricate aligned and tilted Ag nanorod arrays on large substrate areas<sup>25,62–64</sup>. For OAD fabrication, the surface normal of the substrate in a vacuum chamber is positioned at a very large angle with respect to the incoming vapor direction ( $> 75^\circ$ ), as shown in Fig. 2a. This deposition configuration results in a so-called geometric shadowing effect that leads to a preferential growth of nanorods on the substrate in the direction of deposition. The nanorods grow aligned but tilted on the substrate as shown in Fig. 2b. The benefits and limitations of the different methods for preparation of SERS-active substrates are summarized in Table 1.

**Table 1 Comparison of different SERS substrate fabrication techniques that could potentially generate uniform and large area SERS substrates**

Fabrication Method	EBL	NSL <sup>47</sup>	Template method	Hybrid Method	OAD
Enhancement Factor	–	$10^7$ – $10^9$	$10^6$ – $10^7$ (50,52,53)	$10^6$ – $10^8$ (59)	$> 10^8$ (64)
Substrate Area ( $\text{cm}^2$ )	Typically $< 0.001 \times 0.001$	$\sim 1 \times 1$	$> 2.5 \times 2.5$	$> 2.5 \times 5.0$	$> 2.5 \times 7.5$
Uniformity (%)	–	–	$< 15\%$ <sup>50</sup>	–	$< 10\%$ <sup>64</sup>
Reproducibility	$< 20\%$ <sup>38</sup>	–	–	–	$< 15\%$ <sup>64</sup>
Shelf time (days)	–	–	–	$> 40$ (for Au) <sup>60,61</sup>	$\sim 7$ (for Ag)
Fabrication Steps	3	3	3	$> 2$	1–2
Cost	Expensive	Inexpensive	Inexpensive	Inexpensive	Moderate

## Pathogen detection

Several research groups have used these new nanofabrication methods to produce highly sensitive and reproducible SERS substrates for biosensing applications. Studies have been conducted to evaluate SERS quantitatively as a biosensing method for pathogens such as viruses and bacteria<sup>25,28,65–78</sup>. Compared with some of the other pathogen detection techniques previously noted, SERS offers several advantages, including high sensitivity, type and species classification, the discrimination of subtle structural differences, and detection of differences in the nucleic acid profiles between species. We have recently demonstrated that Ag nanorod arrays, produced by oblique angle vapor deposition, offer several advantages for SERS pathogen biosensing applications. While the majority of our applications have been in the area of virus biosensing, we have also demonstrated similar capabilities for the detection of bacteria, as well as other agents including microRNAs, using these Ag nanorod arrays.

### Distinguishing between different virus types

Using the direct intrinsic SERS configuration as shown in Fig. 1a, we have shown that it is possible to rapidly and sensitively distinguish different viruses by their SERS spectra (Fig. 3). For example, the baseline-corrected SERS spectra of the DNA virus, adenovirus (adeno),

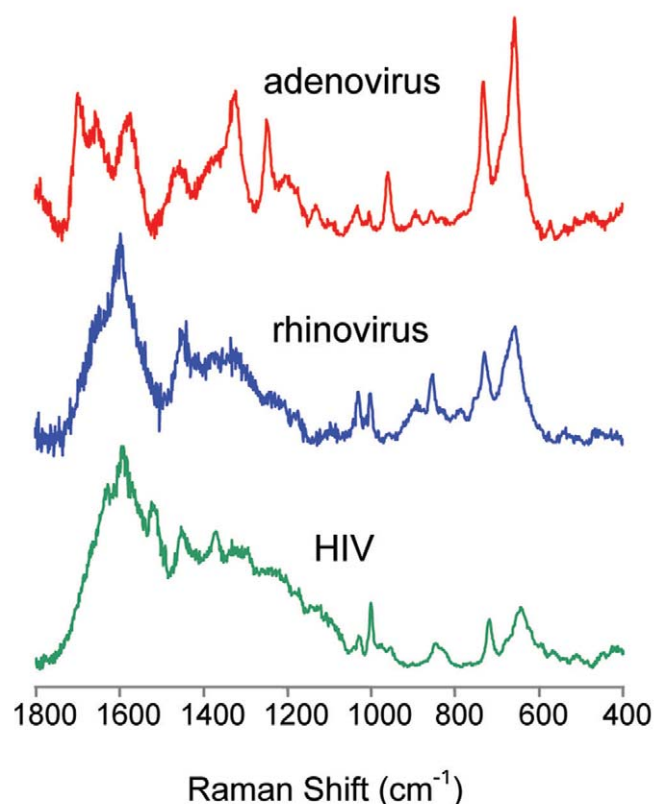


Fig. 3 SERS spectra of different virus types obtained using Ag nanorod substrates. (Reproduced with permission from<sup>25</sup>. © 2006 American Chemical Society.)

and RNA viruses, i.e., rhinovirus (rhino) and human immunodeficiency (HIV) viruses, which can readily be detected and distinguished as shown in Fig. 3. The adeno SERS spectrum is characterized by strong bands due to nucleic acid bases at 650  $\text{cm}^{-1}$  (guanine), 731  $\text{cm}^{-1}$  (adenine), 1325  $\text{cm}^{-1}$  (adenine), and 1248  $\text{cm}^{-1}$  (guanine)<sup>79</sup>. The 650  $\text{cm}^{-1}$  band may also have contributions due to Tyr<sup>80</sup>. The Raman lines at 1003  $\text{cm}^{-1}$  and 1033  $\text{cm}^{-1}$  have been assigned to the symmetric ring breathing mode and the in-plane C-H bending mode of Phe (phenylalanine), respectively<sup>81</sup> while the bands at 1457  $\text{cm}^{-1}$ , 1576  $\text{cm}^{-1}$  and 1655  $\text{cm}^{-1}$  can be attributed to the  $\text{CH}_2$  deformation mode of proteins, the carboxylate stretching vibration ( $\nu_a \text{COO}^-$ ) of Trp (Tryptophan) and the amide I vibration of peptide groups, respectively<sup>81</sup>. A notable characteristic of the adeno SERS spectrum is the relative intensity of the bands associated with the nucleic acids, indicating direct binding to the Ag substrate. The strong band at 731  $\text{cm}^{-1}$  has been assigned to denatured DNA, caused by its interaction with the Ag SERS substrate<sup>82</sup>. A similar band analysis can identify the prominent SERS bands for the other viruses in Fig. 3<sup>25</sup>. Thus, the uniqueness of the SERS spectrum provides a molecular fingerprint for detection of specific viruses and provides the foundation for SERS-based biosensing.

### Detecting viruses in biological media

For most diagnostic situations, the detection of pathogens occurs in a heterogeneous biological medium. Therefore, it is of practical importance that SERS can distinguish between viruses in the presence of a complex background. This capability has been demonstrated by comparing the SERS spectra of uninfected Vero cell lysate, respiratory syncytial virus (RSV) infected cell lysate, and purified RSV (Fig. 4)<sup>25</sup>. As shown in Fig. 4, although there are common SERS peaks for the three samples, both the SERS spectra of RSV-infected cell lysate and purified RSV have SERS bands at 1000–1100  $\text{cm}^{-1}$  and 500–600  $\text{cm}^{-1}$ , while the SERS spectrum of Vero cell lysate does not have these two signature peaks. The bands at 527  $\text{cm}^{-1}$  and 546  $\text{cm}^{-1}$  can be assigned to a disulfide stretching mode<sup>83,84</sup>, while the strong band at 1044  $\text{cm}^{-1}$  has been assigned to the C–N stretching vibration in previous SERS studies<sup>65,85</sup>. The results show that major Raman bands can be assigned to different constituents of the cell lysate and the virus, such as nucleic acids, proteins, protein secondary structure units and amino acid residues present in the side chains and the backbone. However, our most significant result is the observation that vibrational modes due to the virus can be unambiguously identified in the SERS spectrum of the Vero cell lysate after infection.

### Detecting viruses captured onto the nanostructured SERS surface

The indirect intrinsic detection configuration shown in Fig. 1b can also be used to detect viruses captured by antibodies to increase

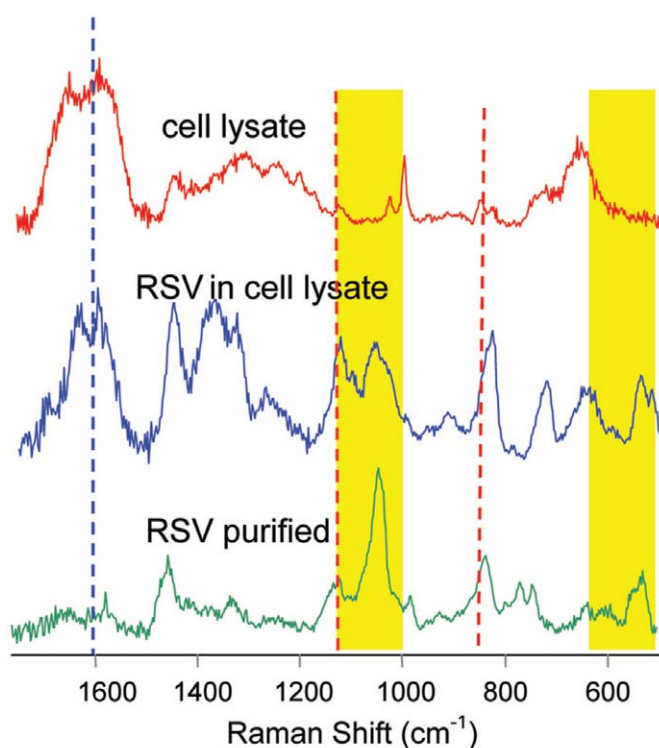


Fig. 4 SERS spectra of Vero cell lysate before and after infection with RSV, top and middle spectra, respectively. The SERS spectrum of purified RSV is shown at the bottom for comparison. (Reproduced with permission from<sup>25</sup>. © 2006 American Chemical Society.)

the detection selectivity. Antibodies can be readily immobilized onto the SERS substrate, and the SERS spectra before and after virus treatment can be obtained to compare Raman signatures of antibody alone versus antibody plus captured virus. The SERS

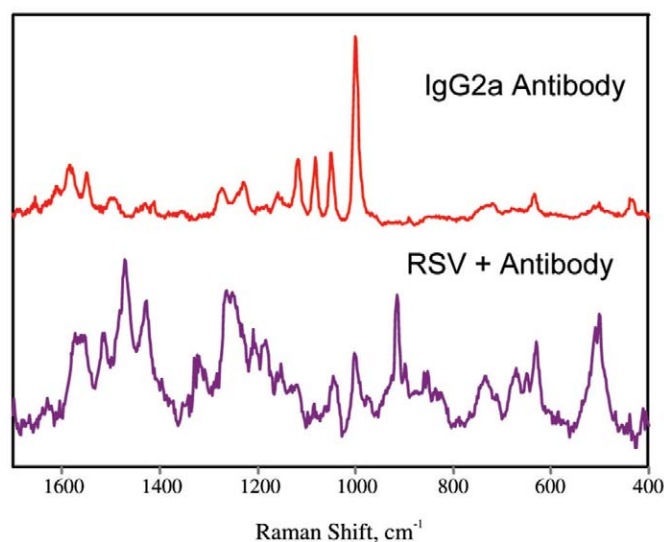


Fig. 5 SERS spectra of (top) IgG2a antibody complex on Ag nanorod array, (bottom) RSV-IgG2a-Ag nanorod complex.

spectra of Ag nanorods coated with the IgG antibodies and viruses captured by these antibodies are shown in Fig. 5. Of the spectral features apparent in the IgG2a antibody spectrum (Fig. 5, top), the most intense band at  $\sim 1000$   $\text{cm}^{-1}$  most likely arises from the in-plane ring deformation mode of Phe in IgG<sup>86,87</sup>. Prominent bands are observed in the 1400–1600  $\text{cm}^{-1}$  region of the RSV and IgG complex spectrum (Fig. 5, bottom). This is presumably due to selectively enhanced nucleic acid and/or side-chain vibrations<sup>88,89</sup>, although the amide III protein mode at  $\sim 1260$   $\text{cm}^{-1}$  may be observed in both the IgG and RSV+IgG spectra<sup>90</sup>. These results show that antibodies or related capture moieties can be used to provide selectivity to SERS biosensing.

### SERS detection of low levels of virus

The sensitivity and dynamic range of the SERS technique for virus detection has been investigated by analyzing dilutions of a respiratory syncytial virus (RSV) mutant lacking the G (attachment) gene ( $\Delta G$ ). The SERS peak areas of the main band at 1045  $\text{cm}^{-1}$  (C–N stretching mode) are plotted against the  $\Delta G$  RSV concentration in Fig. 6<sup>25</sup>. The concentrations of the diluted solutions are calculated from the volume of water used for the dilutions. The SERS intensity increases with concentration of the viral solution, reaching a plateau at concentrations above  $10^3$  PFU/ml (PFU = plaque-forming unit). This behavior is not uncommon and similar findings of decreasing signal with increasing concentration have been reported for SERS substrates with an adsorbate coverage  $\geq 0.01$  monolayer<sup>32</sup>. Although at this stage little emphasis have been placed on determining the lowest detectable titer, values as low as 100 PFU/mL are readily detectable. These data suggest a limit of virus detection ranging from 1–10 PFU of virus in this assay format.

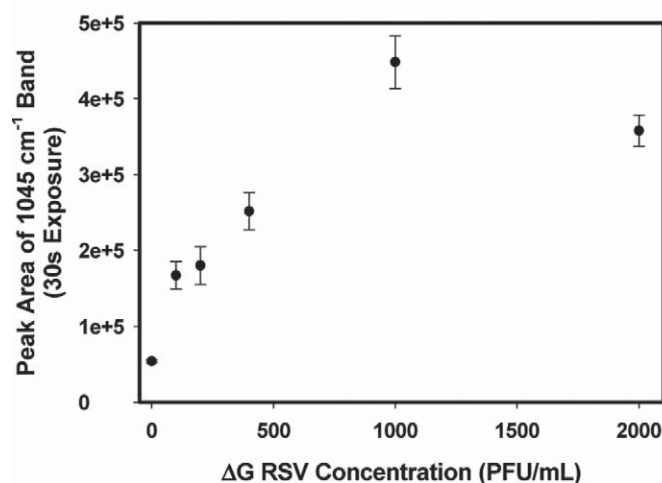


Fig. 6 The SERS calibration curve for  $\Delta G$  RSV constructed with the peak area for the C–N stretching band at 1045  $\text{cm}^{-1}$ . (Reproduced with permission from<sup>25</sup>. © 2006 American Chemical Society.)

### Detecting different strains of a single virus type

In addition to the capacity to differentiate between different virus types, SERS can also be used to distinguish strains of a single virus type<sup>25</sup>. One example is the detection of RSV strains (Fig. 7), although we have also shown that SERS can readily distinguish influenza A strains<sup>25</sup>. Using SERS, the RSV viruses A/Long, A2 and ΔG (belonging to the RSV A strain), as well as the RSV strain B1, have been analyzed and their corresponding baseline corrected spectra (1400 cm<sup>-1</sup>–600 cm<sup>-1</sup>) are shown in Fig. 7.

The SERS spectrum of A/Long (Fig. 7a) differs from the other RSV spectra in that the prominent C–N stretch occurs at 1055 cm<sup>-1</sup>, compared with 1042–1045 cm<sup>-1</sup> for the other RSV viruses. Bands unique to A/Long are also observed at 877 cm<sup>-1</sup> and 663 cm<sup>-1</sup>, while the band at 528 cm<sup>-1</sup> (present in the other spectra) is absent. It is likely that the different spectrum observed for A/Long relates to a different composition of nucleic acids and viral envelope proteins. As predicted, there are also differences in the SERS spectra between the A and B1 strains. The differences that distinguished the A strain from the B strain SERS spectra include the relative intensities of the nucleic acid bands compared with the other bands in the spectrum. Significantly, we have also been able to show that the intrinsic SERS spectra are capable of detecting gene deletions in viruses. This is shown by the SERS spectra comparing the parental A2 strain (Fig. 7d) to the RSV G protein gene deletion mutant from which it

was derived, ΔG (Fig. 7c). Comparison of the spectra reveals subtle yet real differences in peak intensities of the Raman spectra between 700–900 cm<sup>-1</sup>.

### Perspectives

SERS has long been considered as a potential biosensing technology due to its inherently high sensitivity and its ability to provide unique spectroscopic fingerprints of the target analyte. Our recent studies show that, with the appropriate substrate, SERS offers a potent biosensing platform with many advantages over current biosensing or detection applications.

Despite the potential power of SERS as a biosensing tool, there remain critical and practical issues that need to be addressed before the technique can be routinely applied. One consideration is the need to produce inexpensive and reliable SERS substrates having uniformly high enhancements. Another important consideration is the reproducibility of the spectral response from the target biomolecule, which ultimately relates to the statistical reliability of the method. A practical SERS substrate fabrication method would produce an inexpensive, uniform, reproducible, and reusable SERS-active substrate. Since SERS enhancements critically depend on substrate nanomorphology, a practical fabrication method should have the ability to produce nanostructured arrays with specific size, shape, alignment, and architecture within very tight tolerances. Thus, the challenges for a practical SERS nanostructure fabrication method are the ability to:

- (i) control the size, aspect ratio, and shape of nanostructures;
- (ii) grow the desired nanostructure at low temperature and onto a particular substrate geometry, e.g. flat, cylindrical, or tapered;
- (iii) fabricate metallic and dielectric nanostructures in a multilayered fashion; and
- (iv) integrate the fabrication process with other conventional microfabrication techniques.

When considering ultrasensitive SERS detection, e.g. low viral or bacterial loads in a clinical sample, the issue of statistical sampling arises. In such cases, it is possible that when the amount of SERS analyte presents a severe limitation, surface coverage relative to the laser spot size may become an issue in detection. However, this situation may be overcome by employing analyte capture methods, e.g. using antibodies, or by concentrating the limited analyte to be detected. Solutions for these critical issues are addressable and are being investigated so that the door may be opened to a new era of biodetection. **nl**

### Acknowledgments

The authors thank the National Science Foundation, National Institute of Health, Army Research Laboratory, and Georgia Research Alliance for financial support. The authors would also like to acknowledge significant contributions from S. Shanmukh, J. Driskell, L. Jones, J.-G. Fan, V. Chu, Y.-W. Huang, S. Chaney, and Y.-J. Liu.

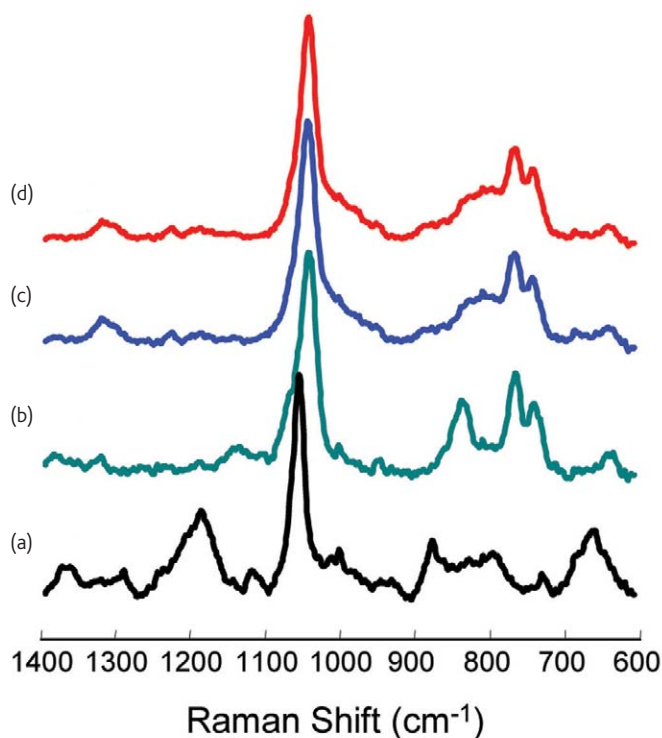


Fig. 7 Summed SERS spectra of individual RSV strains (a) strain A/Long, (b) strain B1, (c), strain A2 with a G gene deletion (ΔG), and (d) strain A2. (Reproduced with permission from<sup>25</sup>. © 2006 American Chemical Society.)

## REFERENCES

- Barenfanger, J., et al., *J. Clin. Microbiol.* (2000) **38**, 2824
- O'Shea, M. K., et al., *Clin. Infect. Dis.* (2005) **41**, 311
- Henkel, J. H., et al., *J. Med. Virol.* (1997) **53**, 366
- Ilic, B., et al., *Appl. Phys. Lett.* (2004) **85**, 2604
- Donaldson, K. A., et al., *Biosens. Bioelect.* (2004) **20**, 322
- Zheng, Y. Z., et al., *J. Virol. Meth.* (1999) **80**, 1
- Kuznetsov, Y. G., et al., *J. Mol. Biol.* (2005) **347**, 41
- Long, D. A., *Raman Spectroscopy*, McGraw-Hill, New York, (1977)
- Fleischmann, M., et al., *Chem. Phys. Lett.* (1974) **26**, 163
- Albrecht, M. G., and Creighton, J. A., *J. Am. Chem. Soc.* (1977) **99**, 5215
- Jeanmaire, D. L., and Van Duyne, R. P., *J. Electroanal. Chem.* (1977) **84**, 1
- Carey, P. R., *Biochemical Applications of Raman and Resonance Raman Spectroscopies*, Academic Press, New York, (1982)
- Campion, A., and Kambhampati, P., *Chem. Soc. Review* (1998) **27**, 241
- Cotton, T. M., and Brandt, E. S., Surface enhanced Raman scattering. In *Physical Methods of Chemistry*, Vol. 9 Rossiter, B.W and Baetzold, R.C (eds), Wiley, New York, (1992).
- Moskovits, M., *Rev. Mod. Phys.* (1985) **57**, 783
- Pemberton, J. E., Surface enhanced Raman scattering. In *Electrochemical Interfaces. Modern Techniques for In-Situ Characterization*, Vol. H. D. Abruna, (eds), VCH Verlag Chemie, Berlin, (1991)
- Weaver, M. J., and Zou, S., Vibrational spectroscopy of electrochemical interfaces: Some walls and bridges to surface science understanding. In *Spectroscopy for Surface Science*, Vol. 26, R. J. H. Clark, and R. E. Hester, (eds), Wiley, Chichester, U.K., (1998)
- Chang, R. K., and Furtak, T. E., *Surface Enhanced Raman Scattering*, Plenum, New York, (1982)
- Ruperez, A., and Laserna, J. J., Surface Enhanced Raman Spectroscopy. In *Modern Techniques in Raman Spectroscopy*, Vol. J. J. Laserna, (eds), Wiley, Chichester, U.K., (1996)
- Moskovits, M., *J. Raman Spectros.* (2005) **36**, 485
- Liang, E. J., and Kiefer, W., *J. Raman Spectros.* (1996) **27**, 879
- Xu, H., et al., *Phys. Rev. Lett.* (1999) **83**, 4357
- Kneipp, K., et al., *Phys. Rev. Lett.* (1997) **78**, 1667
- Premasiri, W. R., et al., *J. Phys. Chem. B* (2005) **109**, 312
- Shanmukh, S., et al., *Nano Lett.* (2006) **6**, 2630
- Qian, X., et al., *Nature Biotechnol.* (2007) **26**, 83
- Kneipp, K., et al., *Appl. Spectrosc.* (2002) **56**, 150
- Driskell, J. D., et al., *Anal. Chem.* (2005) **77**, 6147
- Ahern, A. M., and Garrell, R. L., *Anal. Chem.* (1987) **59**, 2813
- Neddersen, J., et al., *Appl. Spectrosc.* (1993) **47**, 1959
- Xue, G., et al., *Appl. Spectrosc.* (1991) **45**, 756
- Norrod, K. L., et al., *Appl. Spectrosc.* (1997) **51**, 994
- Schlegel, V. L., and Cotton, T. M., *Anal. Chem.* (1991) **63**, 241
- Van Duyne, R. P., et al., *J. Chem. Phys.* (1993) **99**, 2101
- Semin, D. J., and Rowlen, K. L., *Anal. Chem.* (1994) **66**, 4324
- Roark, S. E., and Rowlen, K. L., *Anal. Chem.* (1994) **66**, 261
- Kahl, M., et al., *Sens. Actuators B* (1998) **51**, 285
- De Jesus, M. A., et al., *Appl. Spectrosc.* (2005) **59**, 1501
- Sackmann, M., et al., *J. Raman Spectrosc.* (2007) **38**, 277
- Billot, L., et al., *Chem. Phys. Lett.* (2006) **422**, 303
- Reilly, T. H., et al., *Anal. Chem.* (2007) **79**, 5078
- Alvarez-Puebla, R., et al., *J. Phys. Chem. C* (2007) **111**, 6720
- Hulteen, J. C., et al., *J. Phys. Chem. B* (1999) **103**, 3854
- Jensen, T. R., et al., *J. Phys. Chem. B* (2000) **104**, 10549
- Haynes, C. L., and Van Duyne, R. P., *J. Phys. Chem. B* (2001) **105**, 5599
- Ormonde, A. D., et al., *Langmuir* (2004) **20**, 6927
- Zhang, X., et al., *IEE Proc. Nanobiotechnol.* (2005) **152**, 195
- Yao, J. L., et al., *Pure Appl. Chem.* (2000) **72**, 221
- Kartopu, G., et al., *Phys. Status Solidi A-Applications and Materials* (2006) **203**, R82
- Ruan, C. M., et al., *Langmuir* (2007) **23**, 5757
- Broglin, B. L., et al., *Langmuir* (2007) **23**, 4563
- Gu, G. H., et al., *J. Phys. Chem. C* (2007) **111**, 7906
- Lombardi, I., et al., *Sens. Actuators B* (2007) **125**, 353
- Jung, D. S., et al., *J. Mater. Chem.* (2006) **16**, 3145
- Walsh, R. J., and Chumanov, G., *Appl. Spectrosc.* (2001) **55**, 1695
- Chan, S., et al., *Adv. Mater.* (2003) **15**, 1595
- Lin, H. H., et al., *J. Phys. Chem. B* (2004) **108**, 11654
- Henley, S. J., et al., *Appl. Phys. Lett.* (2006) **89**, 183120
- Chattopadhyay, S., et al., *Chem. Mater.* (2005) **17**, 553
- Suzuki, M., et al., *Appl. Phys. Lett.* (2006) **88**, 203121
- Suzuki, M., et al., *Anal. Sci.* (2007) **23**, 829
- Chaney, S. B., et al., *Appl. Phys. Lett.* (2005) **87**, 31908
- Liu, Y.-J., et al., *Appl. Phys. Lett.* (2006) **89**, 173134
- Driskell, J., et al., *J. Phys. Chem. C* (2008) **112**, 895
- Bao, P. D., et al., *J. Raman Spectrosc.* (2001) **32**, 227
- Isola, N. R., et al., *Anal. Chem.* (1998) **70**, 1352
- Wang, L. Y., et al., *Acta Chimica Sinica* (2002) **60**, 2115
- Sun, B. B., et al., *Biophysical Journal* (2007) **Suppl. S**, 159A
- Liang, Y., et al., *Talanta* (2007) **72**, 443
- Alexander, T. A., and Le, D. M., *Appl. Optics* (2007) **46**, 3878
- Jarvis, R. M., and Goodacre, R., *Anal. Chem.* (2004) **76**, 40
- Zeiri, L., et al., *Appl. Spectrosc.* (2004) **58**, 33
- Jarvis, R., et al., Rapid analysis of microbiological systems using SERS. In *Surface-Enhanced Raman Scattering: Physics and Applications*, Vol. 103, Kneipp, K et. al (eds), (2006)
- Sengupta, A., et al., *Anal. Bioanal. Chem.* (2006) **386**, 1379
- Naja, G., et al., *Analyst* (2007) **132**, 679
- Goeller, L. J., and Riley, M. R., *Appl. Spectrosc.* (2007) **61**, 679
- Liu, Y. L., et al., *Appl. Spectrosc.* (2007) **61**, 824
- Sengupta, A., et al., *Appl. Spectrosc.* (2005) **59**, 1016
- Otto, C., et al., *J. Raman Spectros.* (1986) **17**, 289
- Peticolas, W. L., et al., *J. Raman Spectros.* (1996) **27**, 571
- Podstawka, E., et al., *Appl. Spectros.* (2004) **58**, 570
- Kneipp, K., and Flemming, J., *J. Mol. Struct.* (1986) **145**, 173
- Edwards, H. G. M., et al., *Spectrochim. Acta A* (1998) **54**, 745
- Qian, W. L., and Krimm, S., *J. Raman Spectros.* (1992) **23**, 517
- Stewart, S., and Fredericks, P. M., *Spectrochim. Acta A* (1999) **55**, 1615
- Ljunglof, A., et al., *J. Chromatog. A* (2000) **893**, 235
- Picquart, M., et al., *Biopolymers* (2000) **53**, 342
- Taillandier, E., and Liquier, J., Vibrational spectroscopy of nucleic acids. In *Handbook of Vibrational Spectroscopy*, Vol. 5, J. M. Chalmers and P. R. Griffiths, (eds), Wiley, Chichester, (2002)
- Tuma, R., and Thomas Jr., G. J., Raman spectroscopy of viruses. In *Handbook of Vibrational Spectroscopy*, Vol. 5, J. M. Chalmers and P. R. Griffiths, (eds), Wiley, Chichester, (2002)
- Kitagawa, T., and Hirota, S., Raman spectroscopy of proteins. In *Handbook of Vibrational Spectroscopy*, Vol. 5, J. M. Chalmers and P. R. Griffiths, (eds), Wiley, Chichester, (2002)